Monitoring induced denitrification during managed aquifer recharge in an infiltration pond

A. Grau-Martínez[1], A. Folch[2,3], C. Torrentó[1,4], C. Valhondo[3,5], C. Barba[2,3], C. Domènech[1], A. Soler[1], N. Otero[1,6]*

[1]Grup de Mineralogia Aplicada i Geoquímica de Fluids, Departament de Mineralogia, Petrologia i Geologia Aplicada, SIMGEO UB-CSIC, Facultat de Ciències de la Terra, Universitat de Barcelona (UB), C/ Martí i Franquès, s/n - 08028 Barcelona, Spain. albagrau@ub.edu, clara.torrento@ub.edu, cristina.domenech@ub.edu, albertsoler@ub.edu, notero@ub.edu

[2]Department of Civil and Environmental Engineering (DECA), Universitat Politècnica de Catalunya (UPC), c/Jordi Girona 1-3, 08034 Barcelona, Spain.

[3]Associated Unit: Hydrogeology Group (UPC-CSIC). carme.barba@upc.edu, cristina.valhondo@upc.edu, folch.hydro@gmail.com

[4]Centre for Hydrogeology and Geothermics, University of Neuchâtel, Rue Emile-Argand 11, 2000 Neuchâtel, Switzerland. clara.torrento@unine.ch

[5]Institute of Environmental Assessment and Water Research (IDAEA), CSIC, c/ Jordi Girona 18, 08034 Barcelona, Spain.

[6]Serra Hunter Fellow, Generalitat de Catalunya, Spain.

(*) Corresponding author: Alba Grau-Martínez
e-mail: albagrau@ub.edu, notero@ub.edu
Fax: +34 93 402 13 40.
Phone: +34 93 403 37 73

MONITORING INDUCED DENITRIFICATION DURING MANAGED AQUIFER RECHARGE IN AN INFILTRATION POND

Alba Grau-Martínez[a], Albert Folch[b,c], Clara Torrentó[a,d], Cristina Valhondo[c,e], Carme Barba[b,c], Cristina Domènech[a], Albert Soler[a], Neus Otero[a,f]

Abstract

Managed aquifer recharge (MAR) is a well-known technique for improving water quality and increasing groundwater resources. Denitrification (i.e. removal of nitrate) can be enhanced during MAR by coupling an artificial recharge pond with a permeable reactive layer (PRL). In this study, we examined the suitability of a multi-isotope approach for assessing the long-term effectiveness of enhancing denitrification in a PRL containing vegetal compost. Batch laboratory experiments confirmed that the PRL, installed in 2011, was continuing to enhance denitrification. At the field scale, changes in redox indicators along a flow path and below the MAR-PRL system was monitored over 21 months during recharge (RP) and non-recharge (NRP) periods. Our results showed that the PRL was still releasing non-purgeable dissolved organic carbon five years after installation. Nitrate concentration and isotope data indicated that denitrification was occurring under and close to the infiltration area where recharge water and native groundwater mix. Furthermore, longer operational periods of the MAR-PRL system increased denitrification. Multi-isotope analysis might be useful in identifying and quantifying denitrification in MAR-PRL systems.

Keywords: managed aquifer recharge, multi-isotope analysis, reactive layer, mixing zone, artificial recharge, nitrate isotopes.

1. Introduction

Growing populations with increasing demands for water and potential water shortages require flexible management strategies that replenish aquifers. The artificial recharge of groundwater, commonly known as managed aquifer recharge (MAR), is becoming increasingly important all over the world as a sustainable way of protecting the quality and quantity of groundwater supplies. Recharge ponds are one of the most commonly used approaches for MAR. This approach involves surface infiltration through spreading basins or ponds to introduce surface water into the subsurface environment [Bouwer, 2002; Miller et al., 2006].

Common sources of water for MAR in recharge ponds include wastewater effluents (after different stages of treatment) and effluent-receiving rivers [Díaz-Cruz and Barceló, 2008; Maeng et al., 2011], as well as river water and storm water runoff. These sources of water, mainly those from wastewater treatment plants (WWTPs), might contain high levels of ammonium (NH_4^+), whereas those resulting from agricultural activity might have high concentrations of nitrate (NO_3^-) [Schmidt et al., 2011]. Furthermore, oxic conditions promote ammonium nitrification, transforming it to nitrate.

The chemical composition of the infiltrating water in MAR changes due to a combination of physical and biogeochemical processes as the water passes from unsaturated to saturated zones, where it mixes with native groundwater. In some circumstances, these changes can lead to an overall improvement in groundwater quality [Bouwer, 2002; Fox et al., 2006]. Several studies have demonstrated that artificial recharge reduces the concentration of nutrients [Bekele et al., 2011], organic matter [Bekele et al., 2011; Vanderzalm et al., 2006], metals [Dillon et al., 2006; Bekele et al., 2011], pathogens [Dillon et al., 2006], organic contaminants [Dillon et al., 2006; Patterson et al., 2011] and pharmaceutically active compounds (PhACs) [Herber et al., 2004; Valhondo et al., 2014]. Massmann et al. [2006], investigating changes in redox conditions below an artificial recharge pond in Berlin, found that the level of PhACs in groundwater was controlled by the hydrochemical conditions of

51 the system. Thus, to increase the quality of recharge water and groundwater, the infiltration
52 pond can be coupled to a permeable reactive layer (PRL), an organic reactive layer at the
53 bottom of the pond [Valhondo et al., 2014, 2015, 2016] that promotes diverse redox
54 conditions along the recharge path to enhance the degradation of pollutants.
55 NO_3^- is one of the most abundant pollutants in groundwater [Li et al., 2010; Menció et al.,
56 2016]. Denitrification, a microbe-mediated process in which NO_3^- is converted into dinitrogen
57 gas (N_2), is the main naturally occurring process that decreases NO_3^- concentration in
58 groundwater. Dilution and dispersion also decrease groundwater nitrate concentration, but in
59 contrast to denitrification, they do not lead to mass reduction of the contaminant within an
60 aquifer. Denitrification is carried out by bacteria that use NO_3^- as the terminal electron
61 acceptor when dissolved oxygen (DO), which is energetically more favorable, is unavailable
62 [Knowles, 1982]. Denitrification can be heterotrophic or autotrophic, depending on whether
63 the substrate is organic or inorganic, respectively (Eq.1 and 2).
64 $5CH$ (1)
65 (2)
66 Denitrification can be enhanced in MAR pond systems, since the presence of easily
67 degradable organic carbon, as well as an adequate residence time, promotes the activity of
68 heterotrophic denitrifying bacteria. Recent laboratory studies [Grau-Martínez et al., 2017;
69 Gibert et al., 2008] have suggested that low-cost carbon-releasing materials like organic
70 compost, palm tree leaves and wood by-products could induce denitrification. Promoting
71 denitrification by using a reactive layer in a recharge pond requires control mechanisms to
72 test the efficacy of the implemented materials at the field scale.
73 Multi-isotope analysis, coupled with chemical data, is useful for identifying and even
74 quantifying denitrification processes in aquifers [Mariotti et al., 1988; Aravena and
75 Robertson, 1998; Pauwels et al., 2000, among others]. Denitrification affects the isotope
76 composition of the residual nitrate, resulting in increased levels of the heavy isotopes ^{15}N
77 and ^{18}O [Mariotti et al., 1988; Aravena and Robertson, 1998; Fukada et al., 2003; Kendall et
78 al., 2007]. This change in isotope composition, or isotope fractionation (ε), distinguishes

79 denitrification at the field scale from other processes such as dilution, which can also
80 decrease NO_3^- concentration, but without changing its isotopic value [Clark and Fritz, 1997;
81 Kendall et al., 2007].
82 By combining the analysis of ^{15}N and ^{18}O isotopes with hydrochemical data as well as with
83 the measurement of isotopes of the ions involved in denitrification reactions (e.g., $\delta^{34}S$ and
84 $\delta^{18}O$ of dissolved sulphate and/or $\delta^{13}C$ of dissolved inorganic carbon), additional information
85 on the mechanisms controlling denitrification can be obtained [Aravena and Robertson,
86 1998; Pauwels et al., 1998, 2000, 2010; Kendall et al., 2007; Otero et al., 2009; among
87 others]. Schmidt et al. [2011, 2012] used nitrate isotope ratios to demonstrate the
88 occurrence of denitrification in the infiltrating water during its passage through the first meter
89 of the soil beneath the base of a MAR pond in central coastal California.
90 In the present work, we monitored denitrification processes in a MAR-PRL system located at
91 Sant Vicenç dels Horts, Barcelona, Spain [Valhondo et al., 2014, 2015, 2016], which has a
92 layer of vegetal compost at the bottom of the infiltration pond. The aim of the present study
93 is to test the usefulness of a combined isotope analysis and depth specific hydrochemical
94 data to: (i) assess the long-term effectiveness of the reactive layer in promoting
95 denitrification 5 years after installation; (ii) identify the denitrification processes occurring at
96 different aquifer depths and locations along the saturated zone below the infiltration pond
97 (including the mixing zone between recharge and native groundwater). The field site was
98 monitored during 21 months. Laboratory experiments, using two-year-old vegetal compost
99 from the PRL, were performed to estimate the ε values and, thus, assess the extent of
100 denitrification during MAR. The methods tested here can be applied to assess the efficacy of
101 MAR ponds coupled to reactive layer PRL (MAR-PRL) in promoting denitrification.

102 2. Materials and methods

103 2.1. Site description

The field site studied is located 15 km inland from the Mediterranean coast, in the lower valley of the Llobregat Delta (Catalonia, NE Spain). The aquifer consists of Quaternary alluvial sediments, mainly coarse gravel and sand with small clay lenses [Iribar et al., 1997]. The minerals present include quartz, calcite and dolomite, and the solid phase fraction of organic carbon is less than 0.002 (g_{OC}/g_{soil}) [Barbieri et al., 2011]. At this location, the aquifer extends to a depth of 23 to 27 m underground [Valhondo et al., 2014] and is located between 5 and 10 m below the Llobregat river bed, the river and aquifer thus being hydraulically disconnected [Vázquez-Suñé et al., 2007]. The regional groundwater flow direction is from NNW to SSE [Quevauviller et al., 2009], with a natural hydraulic gradient of 2.3‰. Previous pumping tests determined the hydraulic parameters of the MAR system of Sant Vicenç to be 1.4×10^{4} m^2 day^{-1} for transmissivity and 0.03 for storage coefficient [Barahona-Palomo et al., 2011].

The MAR system in Sant Vicenç dels Horts consists of a decantation pond and an infiltration pond (Fig.1). In the decantation pond (≈4,000 m^2), the sediments are allowed to settle for approximately 2-4 days before the water is transferred by a concrete pipe to an infiltration pond (≈5,000 m^2). The infiltration rate in the infiltration pond ranges from 0.5 to 2 m d^{-1} [Valhondo et al., 2014].

The infiltration water is surface water from the Llobregat River, which is affected by wastewater treatment effluents [Köck-Schulmeyer et al., 2011]. A reactive layer was installed at the bottom of the infiltration pond in 2011 to create favorable conditions for the biodegradation of the contaminants present in the infiltration water. The reactive layer (≈65 cm thick) consists of aquifer sand (49.5% in volume), vegetal compost from gardens and scrap wood (49.5%), clay (≤1%) and iron oxide dust (≤0.1%). The components were mixed on site with an excavator until homogeneity was visually evident. The layer was covered with approximately 5 cm of sand to prevent the woody material from floating away. The compost in the reactive layer was added to promote microbial growth and redox conditions by providing organic matter to the infiltration water. The sand was added to provide structural integrity to the layer and guarantee high hydraulic conductivity. Finally, iron oxides and clay,

consisting mainly of illite (33 wt%), smectite (16 wt%) and chlorite (9 wt%), were present to provide extra sorption capacity for cationic and anionic contaminants [Valhondo et al., 2014].

The MAR pond of Sant Vicenç undergoes two main operational periods: (1) recharge periods (RPs), when the pond is full of the infiltration water and total saturation conditions are not obtained under the infiltration pond [Valhondo et al., 2015, 2016] and (2) non-recharge periods (NRPs), when the pond is emptied for operational redevelopment and/or when the quality of the river water is low. NRPs are implemented when the control parameters of the infiltration water are exceeded, such as when NH_4^+ concentrations are higher than 1.5 mg L^{-1}, electrical conductivity (EC) is higher than 2000 µS cm^{-1}, river turbidity is greater than 100 NTU and input water turbidity exceeds 25 NTU. NRPs are also implemented when the clogged layer needs to be removed or the upper layer of sand has to be cleaned. During NRPs, the groundwater table declines and the bottom of the pond is exposed to the atmosphere.

A piezometric network consisting of seven piezometers was installed around the recharge system of Sant Vicenç dels Horts (Fig.1). Piezometer P1 (screened from 6 to 24 m) is located upstream of the infiltration pond and was used to monitor background groundwater. P3 (screened from 5 to 23 m) is located upstream of the infiltration pond, between the decantation and infiltration ponds, while P8 is located in the middle of the infiltration pond and is composed of three piezometers screened at different depths (P8.1 from 13 to 15 m, P8.2 from 10 to 12 m and P8.3 from 7 to 9 m). P8.3 was used to evaluate the behavior of the infiltration water through the vadose zone, while P8.1 was used to monitor the recharge at the deepest point of the saturated zone. P2 (completely screened from 6 to 24 m) and P5 (screened from 5.5 to 21.5 m) are situated downstream, at the edge of the infiltration pond. Additionally, P9 (9.4-24.4 m) and P10 (6-20 m) are located 190 m and 200 m downstream of the infiltration pond, respectively. Therefore, all the monitoring points, except P1 (native groundwater) and P8.3 (infiltration water just after crossing the vadose zone), represent different ratios of recharge water to native groundwater in the aquifer at different travel times.

159 Travel time of the recharge water to the different piezometers was determined from
160 fluctuations in EC during the infiltration tests [Valhondo et al., 2014]. The results of the
161 infiltration tests were validated by Valhondo et al. [2016] using a numerical model. The
162 results indicated a travel time from the pond to the piezometer of around 18 to 24 hours for
163 P8.3, nearly 2 days for P2 and P5, 10 days for P10 and P8.1, and more than 20 days for P9.

164 **2.2. Sampling surveys**

165 To assess the long-term effectiveness of the PRL on nitrate removal, four sampling
166 campaigns were performed using the seven piezometers (Fig.1) in June 2013, September
167 2013, July 2014 and March 2015. The monitored period started 5 years after the installation
168 of the PRL and lasted 21 months. The June 2013 and July 2014 campaigns were performed
169 during RPs, and the other two during NRPs. Figure 2 shows the distribution along time of the
170 operational periods and the sampling campaigns. The system was under recharge for a total
171 of 222 days in 2013 and 213 days in 2014. In 2015, before the March 2015 campaign, the
172 system was under non-recharge for almost four months, whereas only two months of non-
173 recharge had occurred before the September 2013 campaign.

174 Sampling was carried out using depth-specific samplers (bailers). Bailers are considered
175 suitable for measuring groundwater nitrate concentration (Lasagna and De Luca, 2016).
176 Each piezometer was sampled at three different depths (Fig.1), which were selected
177 according to the stratigraphic profiles. A layer with high transmissivity was identified in the
178 middle depth of all the piezometers. This layer is composed of polygenic gravel and large-
179 sized gravel with medium fine sandy matrix. Although some sampling protocols (ENSAT,
180 2012) do not deem it necessary to purge piezometers in aquifers with high transmissivity
181 such as that of Sant Vicenç dels Horts (1.4×10^{4} m^2 day^{-1}), we still purged the piezometers
182 prior to sampling by removing well water three times at each specific depth. During the four
183 sampling campaigns, samples from the Llobregat River were also collected, sometimes
184 more than once on the same day.

Physicochemical parameters (pH, temperature (T) and EC) were measured *in situ*, using a Multi 3410 multi-parameter (WTW, Weilheim, Germany). Samples for measuring major cations were filtered through 0.2-µm Millipore® filters, preserved by the addition of 1% HNO_3^- and stored in polyethylene bottles at 4ºC until analysis. Samples for the analysis of major anions (Cl^-, NO_3^-, NO_2^- and SO_4^{2-}) and isotope ratios ($\delta^{15}N_{NO3}$, $\delta^{18}O_{NO3}$, $\delta^{34}S_{SO4}$, $\delta^{18}O_{SO4}$ and $\delta^{13}C_{HCO3}$) were filtered through 0.2-µm Millipore® filters and stored in polyethylene bottles. Samples for measuring NO_3^- isotopes were kept frozen until analysis, while those for $\delta^{18}O_{H2O}$ and $\delta^{2}H_{H2O}$ measurements were collected in glass flasks and filtered through 0.45-µm Millipore® filters. For isotope analyses, samples were taken only from the middle depth of each piezometer. Samples for the analysis of non-purgeable dissolved organic carbon (NPDOC) were collected in muffled (450°C, 4.5 hours) glass bottles, filtered through 0.45-µm Millipore® filters, acidified to pH 3 with hydrochloric acid and stored at 4°C until analysis. To measure dissolved inorganic carbon (DIC), samples were collected in glass bottles, filtered through 0.45-µm Millipore® filters and analyzed within a day.

2.3. Laboratory experiments

Batch experiments were performed with material extracted in 2013 from the PRL of the Sant Vicenç dels Horts MAR pond system. The substrate was used within a few hours after extraction without any pre-treatment. Total N and C content as well as the $\delta^{15}N$ and $\delta^{13}C$ of the reactive layer material are shown in the Supplementary Material (Table S1). Experiments were performed in triplicate, using 20 g of the PRL material and 400 mL of groundwater from the Llobregat aquifer (from P2) spiked with 0.80 mM of NO_3^- to evaluate the denitrification potential of the vegetal compost. The experiments were run in sterilized 500-mL glass bottles previously purged with N_2 for 15 minutes in a glove box in an argon atmosphere to minimize the O_2 level. Experimental oxygen partial pressure in the glove box was maintained between 0.1 and 0.3% O_2 and continuously monitored using an oxygen partial pressure detector (Sensotran, Gasvisor 6) with an accuracy of ± 0.1% O_2. Batch experiments were manually shaken once a day and aqueous samples (5 mL) were collected daily using

sterilized syringes. A ratio of solution/solid material at 90% of the initial value was maintained.

2.4. Analytical methods

Concentrations of major anions was determined by high performance liquid chromatography (HPLC) using a WATERS 515 HPLC pump, an IC-PAC anions column and a WATERS 432 detector. Cation concentrations were determined by inductively coupled plasma-optical emission spectrometry (ICP-OES, Perkin-Elmer Optima 3200 RL). NPDOC was measured by organic matter combustion using a MULTI N/C 3100 Analytik Jena carbon analyzer. DIC concentrations were analyzed by titration (METROHM 702 SM Titrino). Chemical analyses were conducted at the “Centres Científics i Tecnològics” of the University of Barcelona (CCiT-UB).

The $\delta^{15}N$ and $\delta^{18}O$ isotopes of dissolved NO_3^- were measured using a modified cadmium reduction method of McIlvin and Altabet [2005] and Ryabenko et al. [2009]. Briefly, NO_3^- was converted into nitrite through a spongy cadmium reduction and then to nitrous oxide using sodium azide in an acetic acid buffer. Simultaneous $\delta^{15}N$ and $\delta^{18}O$ analysis of the N_2O produced was carried out with a PreCon system (Thermo Scientific) coupled to a Finnigan MAT-253 Isotope Ratio Mass Spectrometer (IRMS, Thermo Scientific). For $\delta^{34}S$ and $\delta^{18}O$ analyses, dissolved SO_4^{2-} was precipitated as $BaSO_4$ by adding $BaCl_2$ after acidifying the sample with HCl and boiling it to prevent $BaCO_3$ precipitation, following standard methods [Dogramaci et al., 2001]. $\delta^{34}S$ was analyzed with a Carlo Erba elemental analyzer (EA)-Finnigan Delta C IRMS, while $\delta^{18}O$ was analyzed in duplicate with a ThermoQuest high temperature conversion EA (TC/EA) coupled in continuous flow with a Finnigan MAT Delta C IRMS. For $\delta^{13}C_{DIC}$ analysis, carbonates were precipitated by adding a NaOH-$BaCl_2$ solution and isotope ratio was measured on a Gas-Bench II-MAT-253 IRMS (Thermo Scientific). $\delta^{2}H_{H2O}$ and $\delta^{18}O_{H2O}$ were analyzed by Wavelength-Scanned Cavity Ringdown Spectroscopy (WS-CRDS) using L2120-i Picarro®. Total C, total N, $\delta^{15}N$ and $\delta^{13}C$ from the PRL material

were measured using Carbo Erba EA-Finnigan Delta C IRMS. Isotope ratios were calculated using both international and internal laboratory standards. Notation was expressed in terms of δ relative to the international standards (V-SMOW for $\delta^{18}O$ and $\delta^{2}H$, atmospheric N_2 for $\delta^{15}N$, V-CDT for $\delta^{34}S$ and V-PDB for $\delta^{13}C$). The reproducibility of the samples was ±1‰ for the $\delta^{15}N$ of NO_3, ±1.5‰ for the $\delta^{18}O$ of NO_3^-, ±0.2‰ for the $\delta^{34}S$ of SO_4^{2-}, ±0.5‰ for the $\delta^{18}O$ of SO_4^{2-}, ±0.2‰ for the $\delta^{13}C$ of DIC, ±0.2‰ for the $\delta^{18}O$ of H_2O and ±1‰ for the $\delta^{2}H$ of H_2O. Samples for isotopic analyses were prepared at the "Mineralogia Aplicada i Geoquímica de Fluids" laboratory and analyzed at CCiT-UB, except water isotopes, which were analyzed at the University of Málaga.

3. Results and discussion

Results from the batch experiments and the complete chemical and isotopic characterization of the field samples are detailed in the Supplementary Material (Table S2 and Tables S3, respectively).

3.1. Laboratory experiments

Complete NO_3^- reduction was achieved within eleven days in the batch experiments (Fig. 3), with a slight transient increase in NO_2^- concentration (up to 0.07 mM). Nitrate reduction in previous batch experiments performed with fresh commercial compost was accompanied by a significant initial release of NO_3^- (up to 2.5 mM) and transient NO_2^- production (up to 0.12 mM) [Grau-Martínez et al., 2017]. By comparison, the compost used in the present batch experiments, extracted from the PRL two years after its installation, did not release NO_3^- and produced a lower increase in NO_2^- concentration.

Denitrification in both sets of batch experiments followed pseudo-first-order kinetics and an initial lag phase of 6-7 days with a lower degradation rate was observed. The pseudo-first order degradation rate constant (k'), calculated using Eq. 3 (where C_0 and C_t are the initial NO_3^- concentration and the NO_3^- concentration at time t, respectively, in mmol L^{-1}), were

263 0.21±0.01 and 0.83±0.06 d^{-1} with the PRL material and 0.17±0.02 and 0.67±0.01 d^{-1} with the
264 fresh compost for the lag and main phases, respectively. Although highly similar, degradation
265 rates were slightly higher for the PRL material than for the fresh compost. These results
266 demonstrated that the compost from the PRL still had denitrification potential two years after
267 its installation.

268 = (3)

269 The isotope fractionation factor α can be obtained [Mariotti et al., 1988; Aravena and
270 Robertson, 1998] according to Eq. (4), assuming a Rayleigh distillation process:

271 ln(—)=(ln (—) (4)

272 where R_o and R_t denote the ratios of heavy to light isotopes at the initial time and time t,
273 respectively, which are calculated according to Eq. (5).

274 —— (5)

275 The term (α -1) was calculated from the slope of the regression line in the double-logarithmic
276 plots [$\ln(R_t/R_0)$] vs. [$\ln(C_t/C_0)$], according to Eq. (4), and converted into isotope fractionation
277 (εN and εO) following Eq. (6).

278 (6)

279 The isotopic fractionations obtained were -10.4‰ for εN and -13.8‰ for εO, with a εN/εO
280 ratio of 0.75 (Fig. 4). The εN and εO values obtained in this study were similar to those from
281 previous laboratory experiments using fresh commercial compost (εN= -10.8‰ and εO=-
282 9.0‰ [Grau-Martínez et al., 2017]), also falling within the range of laboratory values for
283 heterotrophic denitrification reported in the literature (from -8.6‰ to -16.2‰ for εN and from -
284 4‰ to -13.8‰ for εO [Knöller et al., 2011; Carrey et al., 2013]).
285 The obtained C and N isotope fractionations associated with denitrification induced by the

two-year-old PRL material enables a more accurate quantification of the enhanced reduction in NO_3^- levels in the aquifer.

3.2. Field study

3.2.1. Hydrochemical characterisation

For all the analyzed samples, pH values ranged between 6.98 and 7.60, HCO_3^- concentrations between 223 and 408 mg L^{-1} and EC from 991 to 1653 μS cm^{-1}. There were no significant differences in the concentrations of major cations between the piezometers among the four sampling campaigns (Table S3).

Groundwater underneath the infiltration pond can be considered a mixture of recharge water and native groundwater. Samples clustered in the HCO_3-Cl-Ca-Na hydrochemical facies, with negligible differences among the sampling campaigns (data not show). The saturation index of calcite, calculated using the PHREEQC code [Parkhurst and Appelo, 2012] and the LLNL.dat database, ranged from -0.35 to 0.6, indicating that calcite was in equilibrium with native groundwater and had a pH buffering role in the hydrochemistry of the aquifer among the Quaternary alluvial sediments.

3.2.2. Sources of groundwater recharge

δ^2H and $\delta^{18}O$ values of the infiltration water (river water) and groundwater sampled during RPs (June 2013 and July 2014) mostly plotted along the Local Meteoric Water Line (LMWL) (Fig. 5). The LMWL was calculated with data from the Global Network of Isotopes in Precipitation (GNIP) obtained from stations 0818001 and 0818002 in Barcelona (IAEA/WMO, 2017). Isotope ratios are lower than the weighted mean long-term isotopic composition of precipitation in Barcelona (δ^2H= -31.16‰, $\delta^{18}O$= -5.3‰), but in agreement with the values obtained with the surface water of the Lower end of the Llobregat River [Otero et al., 2008] and samples from the Llobregat aquifer [Solà, 2009]. The results confirmed that river water is the main source of recharge in the aquifer and indicate that evaporation is not an important process in the pond and/or the unsaturated zone. Lastly, the

312 range of $\delta^{2}H$ and $\delta^{18}O$ values showed that only one recharge flow system is involved in the
313 aquifer recharge.

314 **3.3. Changes in redox sensitive indicators**

315 The evolution of the concentration of NO_3^- and NPDOC in the saturated zone along the flow
316 path, during both RPs and NRPs, is shown in Figure 6. The results of major anions (Cl^-,
317 SO_4^{2-}, HCO_3^-) are shown in the Supplementary Material (Fig. S1).

318 The chemical composition of groundwater collected upstream of the infiltration pond (P1,
319 which represents native groundwater not affected by the recharge) was compared to that of
320 the piezometers affected by recharge water. The concentrations of major anions in P1
321 samples remained almost constant with depth and time, although SO_4^{2-} and Cl^-
322 concentrations were slightly lower in June 2013 (Fig. S1). As expected, the influence of river
323 water hydrochemistry is clearly observed during RP in the piezometers located closer to the
324 infiltration pond (P8, P2 and P5) and is observed to a lesser extent during NRP. Significant
325 changes with depth are only detected in P8 that showed increasing HCO_3^- concentrations
326 with depth, except in July 2014 (RP). Piezometers located furthest from the infiltration pond
327 (P9 and P10) are less influenced by river water chemistry, showing values similar to P1 and
328 P3, and no significant changes with depth were observed during both RP and RNPs.

329 During RPs, NPDOC concentrations at all the piezometers downstream of the infiltration
330 pond generally ranged between those for native groundwater (1.9-4.9 mg L^{-1}) and those for
331 river water (3.2-3.7 mg L^{-1}), except the higher values measured in the shallowest part of P5
332 in June 2013 (4.1 mg L^{-1}) and the deepest part of P2 in July 2014 (5.5 mg L^{-1}) (Fig. 6).
333 During NRPs (September 2013 and March 2015), NPDOC concentration in most of the
334 mixed groundwater samples also ranged between those for native groundwater (1.9-3.0 mg
335 L^{-1}) and those for river water (4.3-4.7 mg L^{-1}), being generally lower than the values obtained
336 from the RPs. Higher concentrations were detected in September 2013 than in March 2015,
337 especially for the shallowest part of P3 (8.6 mg L^{-1}) and the deepest part of P8 (7.1 mg L^{-1}).

These results suggest that the reactive layer was still releasing NPDOC five years after installation. The effects of the PRL was more apparent at P2 and P5 during RPs and especially P3 and P8 during NRPs. Higher levels of organic matter were released from the PRL during September 2013 (two months of non-recharge before sampling) than March 2015 (four months of non-recharge before sampling), indicating that the duration of recharge conditions had a significant effect.

During the monitoring period, NO_3^- concentration in native groundwater (P1) ranged from 4.1 to 6.4 mg L^{-1}, except the higher values recorded in March 2015 (9.8 mg L^{-1}) and September 2013 (3.7-6.9 mg L^{-1}) (Table S3). Similarly, NO_3^- contents in river water ranged from 6.1 to 8.4 mg L^{-1}. It should be noted that NO_3^- and NH_4^+ concentrations vary considerably in rivers with effluents from WWTPs, even among samples collected on the same day. During the RPs a significant decrease in NO_3^- concentration was observed in the piezometers located close to the infiltration pond (P2 and P5), especially in the June 2013 sampling, which showed complete NO_3^- reduction at some depths highlighting the ability of the MAR-PRL system to enhance nitrate reduction (Fig.6). Low NO_3^- concentration also occurred in the shallowest part of P8 (0.9 mg L^{-1}), increasing with depth probably because P8.3 is more affected by the recharge water than P8.2 and P8.1. During the July 2014 RP, although NO_3^- concentration in the mixed groundwater was lower than that in the native groundwater, higher values and smaller changes with depth and along the flow path were observed. During NRPs, NO_3^- concentrations at the piezometers downstream of the infiltration pond were generally within native groundwater and river water samples, although slightly lower NO_3^- concentrations were detected at P2, suggesting that NO_3^- reduction was maintained to some extent during NRPs.

Fe concentrations in samples downstream of the infiltration pond were generally lower than that in the native groundwater (P1) (data not shown). No significant variations between the sampling campaigns were observed (values ranged from 0.2 to 1.0 µM at all the piezometers and depths studied), except for an important increase at P5 during the June

2013 RP (up to 3.7 µM) probably arising from more reducing conditions occurring. The solubility of Fe(III)-oxyhydroxides, which usually affects Fe concentration in groundwater, increases under more reducing conditions, thereby increasing aqueous Fe concentration.

Overall, the observed changes in redox indicators suggested that the PRL installed in 2011 was still releasing organic matter and promoting reducing conditions to varying extents below the infiltration pond.

3.4. Denitrification during artificial recharge

Samples for isotope analyses were taken only from the middle depth of each piezometer. Nitrate isotope composition was measured in a subset of these samples based on NO_3^- concentrations. Figure 7 shows the $\delta^{15}N_{NO3}$ and $\delta^{18}O_{NO3}$ values of dissolved nitrate at the piezometers, as well as the isotope composition of the main potential sources of nitrate: nitrate fertilizers, ammonium fertilizers, soil nitrate and animal manure or sewage [Vitòria et al., 2004; Kendall et al., 2007; Xue et al., 2009]. The range of $\delta^{18}O$ of NO_3^- for ammonium fertilizers, soil nitrogen and manure/sewage plotted in Figure 7 (+1.93‰ to +3.13‰) was estimated according to Eq.7 [Anderson and Hooper, 1983; Kendall et al., 2007], where $\delta^{18}O_{H2O}$ corresponds to the range measured in Sant Vicenç dels Horts groundwater samples and $\delta^{18}O_{O2}$ to atmospheric O_2 (+23.5‰ [Horibe et al., 1973]).

– – (7)

Native groundwater (P1) showed $\delta^{15}N$ and $\delta^{18}O$ values ranging from +13.0 to +17.5‰ and from +2.8 to +9.7‰, respectively. The nitrate isotope ratios of the samples from the piezometers located downstream of the pond ranged from +9.5 to +26.7‰ (averaging +18.4‰) for $\delta^{15}N$ and from +3.5 to +16.6‰ (averaging +9.5‰) for $\delta^{18}O$ (Table S4). All these samples presented isotope ratios compatible with those for soil organic nitrogen and sewage/manure. The mixed groundwater samples showed a positive correlation (r^2=0.55) between $\delta^{15}N_{NO3}$ and $\delta^{18}O_{NO3}$ and were aligned following a εN/εO ratio of 1.5 (Fig. 7), which is consistent with denitrification [Kendall et al., 2007]. The εN/εO ratio reported in the

391 literature for denitrification in groundwater ranges from 1.3 to 2.1 [Böttcher et al., 1990; Cey
392 et al., 1999; Mengis et al., 1999; DeVito et al., 2000; Lehmann et al., 2003; Fukada et al.,
393 2003].

394 The lowest NO_3^- concentrations in groundwater were measured in the samples obtained
395 during the June 2013 RP, with those recorded in P2 and P5 samples being close to the
396 detection limit at most of the depths studied (Fig. 6), thus suggesting denitrification. For the
397 June 2013 samples in which NO_3^- content was high enough for isotope characterization,
398 $\delta^{15}N$ and $\delta^{18}O$ values were up to +21.0‰ and +9.5‰, respectively (Fig. 7). Whereas the P8
399 and P9 samples followed a trend consistent with denitrification, the samples P2 and P10 do
400 not fit to the denitrification trend. These samples likely correspond to denitrification of NO_3^-
401 resulting from the nitrification of the ammonium in sewage that had undergone further
402 volatilization. In this sampling campaign, all the piezometer samples, except the middle and
403 deepest part of P8, showed lower NO_3^- concentrations than native groundwater and river
404 water (Fig. 6). The middle part of P8 showed similar nitrate isotope ratios as P1 and river
405 water (Fig. 7).

406 Native and mixed groundwater samples from the July 2014 RP campaign gave higher $\delta^{15}N$
407 and $\delta^{18}O$ values than those from the June 2013 RP campaign (Fig. 7). Nevertheless, $\delta^{15}N$
408 and $\delta^{18}O$ values (up to +25.3‰ and +16.1‰, respectively) were higher in all the mixed
409 groundwater samples than in native groundwater (+18.8‰ and +11.4‰, respectively), which
410 is consistent with denitrification. The exception was the P10 sample (+19.1‰ and +10.9‰,
411 respectively), which showed similar isotope ratios as P1. The highest $\delta^{15}N$ and $\delta^{18}O$ values
412 were measured in P2 (+25.3‰ and +16.1‰, respectively). However, it should be noted that
413 high $\delta^{15}N$ and $\delta^{18}O$ values were also measured in river water. The high variability in NO_3^-
414 contents in river water samples even on the same day (data not shown) could explain the
415 particularly high isotope ratios measured in September 2013 and July 2014.

416 All the mixed groundwater samples, except P2, collected during the March 2015 NRP (when

417 the pond had been under non-recharge for four months) showed similar isotope ratios as the
418 native groundwater (P1, $\delta^{15}N$= +13.9‰ and $\delta^{18}O$= +5.6‰). Those collected in the
419 September 2013 NRP, when the pond had been under non-recharge for a shorter time (two
420 months), showed higher $\delta^{15}N$ and $\delta^{18}O$ values than P1 (+17.5‰ and +9.7‰, respectively),
421 except P5 and P8 samples (Fig. 7). In both sampling surveys, P2 samples presented the
422 highest isotope ratios ($\delta^{15}N$ and $\delta^{18}O$ were +17.3‰ and +9.3‰ in March 2015 and +26.7‰
423 and +16.6‰ in September 2013, respectively). Thus, differences between the two NRP
424 sampling campaigns indicate that the effect of the RP can take some time to manifest after
425 non-recharge conditions.

426 εN and εO values allow quantifying at field scale NO_3^- losses due to denitrification
427 independently of dilution effects on NO_3^- concentrations [Mariotti et al., 1981; Böttcher et al.,
428 1990; Fukada et al., 2003; Otero et al., 2009; Torrentó et al., 2011]. With the ε values
429 obtained in laboratory experiments, the percentage of denitrification at the field scale can be
430 calculated according to Eq. 8 using either εN or εO, or both.

431 (8)

432 Using the ε values obtained in the batch experiments with the two-year-old PRL material (-
433 10.4‰ for εN and -13.8‰ for εO, with an εN/εO ratio of 0.75) and assuming an initial isotope
434 composition similar to that of the P1 samples collected in June 2013 ($\delta^{15}N_{NO3}$= +13.0‰ and
435 $\delta^{18}O_{NO3}$= +2.8‰) (corresponding to the lowest values measured), the extent of denitrification
436 ranged from 0% to 50%, except for two samples (P2 in September 2013 and July 2014)
437 showing reductions greater than 60% (Fig. S2). The median percentage of NO_3^- reduction in
438 groundwater was 36±22% (n=19) when using the laboratory-obtained εN and 32±19% (n=
439 20) when using εO.

440 A more precise estimation of the extent of denitrification enhanced by the MAR-PRL system
441 in the mixed groundwater samples was determined for each sampling campaign using the

442 isotope composition of the native groundwater (P1) for each campaign as the initial value. It
443 should be noted that P1 and river samples collected in July 2014 (RP) and September 2013
444 (NRP) showed high values of $\delta^{15}N$ and $\delta^{18}O$, indicating the occurrence of natural
445 attenuation. High NO_3^- concentrations indicate other sources of NO_3^- (such as fertilizers from
446 the fields around Sant Vicenç dels Horts). Compared to native groundwater, P9 and P10
447 (located furthest from the infiltration pond) samples, except those collected in the June 2013
448 RP (NO_3^- reduction of around 30%), presented the lowest level of denitrification (NO_3^-nitrate
449 reduction less than 10%). Denitrification was enhanced in the piezometers located closer to
450 the infiltration pond (P2 and P5). For P5, the degree of reduction in NO_3^- concentration was
451 greater in RPs (around 15%) than in NRPs (no denitrification); however, this difference was
452 not so significant for P2 (30-35% vs. 25-45%, respectively). In all the campaigns, the isotope
453 composition of P8.2 was very similar to that of P1, indicating that denitrification was not
454 occurring at this depth. Since isotope values in samples from different depths were not
455 determined, the observed variations in NO_3^- concentration with depth at P8 cannot be
456 attributed to denitrification or other process (e.g., mixing).

457 Therefore, denitrification occurred during both RPs, the maximum degree of attenuation
458 (between 30 and 40%) taking place at the middle depths of P2 and P5. Complete
459 denitrification at some of the depths of P2 and P5 was observed in samples collected in
460 June 2013 (Fig. 6). Comparing the two RP sampling campaigns, the June 2013 samples
461 presented a slightly higher level of denitrification, probably because the system was under
462 almost continuous operation since January 2012 (except for 30 days in August 2012, 24
463 days in February-March 2013 and 5 days in April 2013). The MAR system was stopped from
464 22nd June to 1st July, 10 days before the July 2014 sampling campaign. The longer
465 operational period before the June 2013 campaign could have induced a well-developed
466 denitrifying microbial community, with the bacteria being more concentrated in the areas
467 receiving more recharge water, such as P2 and P5. Li et al. [2013], simulating the infiltration
468 zone of a MAR system, showed that microbial communities reached stability after 3-4

months of operation.

During NRPs, the percentage of denitrification was very low (<20%) in all the samples, except those from P2 (30-60%), which was one of the areas most affected by recharge water (Valhondo et al., 2014) (Fig. 8). All the samples collected in March 2015, including P2, showed the lowest percentage of denitrification among all the sampling campaigns. The September 2013 campaign was performed after a year of almost continuous recharge (Fig. 2) followed by less than two months of non-recharge, whereas the March 2015 campaign was undertaken after almost four months of non-recharge. Differences in the percentage of denitrification among the P2 samples collected from both NRPs indicate that the bacteria grow during RPs were still denitrifying even when the MAR pond was under non-recharge, but became less active with time in the absence of a carbon source [Rodríguez-Escales et al., 2016].

3.5. Additional isotope data

The isotope composition of SO_4^{2-} ($\delta^{34}S_{SO4}$ and $\delta^{18}O_{SO4}$) was analyzed to assess the occurrence of sulfate-reducing conditions. The isotope composition of the dissolved SO_4^{2-} in mixed groundwater samples was only analyzed for the June 2013 and September 2013 campaigns. Values ranged from +6.7 to +10.6‰ for $\delta^{34}S$ and from +9.0 to +11.1‰ for $\delta^{18}O$ (Fig. 9). Similar values were obtained for the river water and native groundwater samples. Most of the mixed groundwater samples gave values within the range obtained for sewage [Otero et al., 2008] (Fig. 9), indicating that the vast majority of SO_4^{2-} came from sewage, which is consistent with the conclusions drawn from the NO_3^- isotope results regarding potential NO_3^- sources.

The narrow range of the $\delta^{34}S_{SO4}$ and $\delta^{18}O_{SO4}$ values obtained suggests a lack of SO_4^{2-} reduction. Based on these results and those from the NO_3^- isotope analysis, it can be concluded that the NPDOC released by the reactive layer produces variable redox

494 conditions in the saturated zone along the flow path, leading mainly to the reduction of NO_3^-,
495 as well as iron under certain conditions, but not of SO_4^{2-}.
496 Due to the lithology of the aquifer, native groundwater contained high concentrations of
497 natural bicarbonate (median value of 325±25 mg L^{-1} in P1 for the four sampling campaigns)
498 that could buffer any change in the $\delta^{13}C_{HCO3}$ isotope ratio. The $\delta^{13}C_{HCO3}$ values in P1 samples
499 (native groundwater) averaged -13.2±1‰, which is in agreement with the known range of
500 $\delta^{13}C_{HCO3}$ for groundwater (-16‰ to -11‰ [Vogel and Ehhalt, 1963]). Mixed groundwater
501 samples displayed $\delta^{13}C_{HCO3}$ values close to that of P1 samples (between -13.8 and -12.0‰,
502 with a median value of -12.7‰), except three samples collected in the June 2013 campaign
503 (RP) (that had values ranging from -11.1 to -9.9‰) (Fig. 10). As expected, the role of organic
504 matter oxidation in the observed denitrification processes was not evident from the $\delta^{13}C_{HCO3}$
505 data due to the buffering effect of the bicarbonate.

506 **4. Conclusions**

507 We evaluated the feasibility of a multi-isotope approach for assessing the efficacy of the
508 MAR-PRL system of Sant Vicenç dels Horts in promoting denitrification in the groundwater
509 below the infiltration pond. Similarities in the hydrochemical data (except for NO_3^- levels,
510 which decreased during recharge periods) of river water, native groundwater and mixed
511 groundwater demonstrated a unique recharge flow system. Changes in the redox indicators
512 with depth and along the flow path during recharge and non-recharge periods confirmed that
513 the reactive layer was still releasing NPDOC five years after installation. NO_3^- concentrations
514 decreased during recharge periods especially in the piezometers closest to the infiltration
515 pond, while aqueous Fe concentrations increased in the piezometers with lower NO_3^-
516 concentrations. However, SO_4^{2-} reduction was not observed.

517 Isotope data revealed that denitrification occurred in the area under the infiltration pond. The
518 piezometers closest to the MAR-PRL, P2 and P5, showed higher levels of denitrification

than the other piezometers. Importantly, denitrification was enhanced by a more continuous recharge of the MAR-PRL system, probably because microbial communities become stable after 3-4 months of continuous operation. Although a more detailed field sampling survey is needed to determine the real extent of denitrification at the field scale, the results of this study show the usefulness of a multi-isotope approach in identifying denitrification in MAR-PRL systems.

Acknowledgements

This study was funded by the projects REMEDIATION [Spanish Government, ref. CGL2014-57215-C4-1-R], MAG [Catalan Government, ref. 2014SGR-1456], WADIS-MAR [Water Harvesting and Agricultural Techniques in Dry Lands: an Integrated and Sustainable Model in Maghreb Regions, European Commission, ref. ENPI/2011/280-008] and the European Union project MARSOL [FP7-ENV-2013-WATER-INNO-DEMO].

References

Anderson, K.K., Hooper, A.B., (1983). O_2 and H_2O are each the source of O in NO_2 produced from NH_3 by Nitrosomas ^{15}N-NMR evidence. FEBS Lett. 64, 236-240.

Aravena, R., Robertson, W.D., (1998). Use of multiple isotope tracers to evaluate denitrification in ground water: Study of nitrate from a large-flux septic system plume. Ground Water 36, 975-982.

Barahona-Palomo, M., Barbieri, M., Fernàndez-Garcia, D., Pedretti, D., Sanchez-Vila, X., Valhondo, C., Queralt, E., Massana, J., Hernández, M., Tobella, J., (2011). Caracterització del Sistema de Recàrrega de Sant Vicenç dels Horts: Projecte RASA, Informe Fase 2, Barcelona: CUADLL.

Barbieri, M., Carrera, J., Sanchez-Vila, X., Ayora, C., Cama, J., Köck-Schulmeyer, M., López de Alda, M., Barceló, D., Tobella Brunet, J., Hernández García, M., (2011). Microcosm experiments to control anaerobic redox conditions when studying the fate of organic micropollutants in aquifer material. J. Contam. Hydrol. 126 (3-4): 330-345.

545 Bekele, E., Toze, S., Patterson, B., Higginson, S., (2011). Managed aquifer recharge of
546 treated wastewater: water quality changes resulting from infiltration through the vadose
547 zone. Water Res. 45 (17), 5764-5772.

548 Böttcher, J., Strebel, O., Voerkelius, S., Schmidt, H.L., (1990). Using isotope fractionation of
549 nitrate-nitrogen and nitrate-oxigen for evaluation of microbial denitrification in sandy aquifer.
550 J. Hydrol. 114, 413-424.

551 Bouwer, H., 2002. Artificial recharge of groundwater: hydrogeology and engineering.
552 Hydrogeol. J. 10, 121-142.

553 Carrey, R., Otero, N., Soler, A., Gomez-Alday, J.J., Ayora, C., (2013). The role of Lower
554 Cretaceous sediments in groundwater nitrate attenuation in central Spain: Column
555 experiments. Appl. Geochem. 32, 142-152.

556 Cey, E.E., Rudolph, D.L., Aravena, R., Parkin, G., (1999). Role of the riparian zone in
557 controllingthe distribution and fate of agricultural nitrogen near a small stream in southern
558 Ontario. J. Contam. Hydrol. 37, 45-67.

559 Clark, I.D., Fritz, P., (1997). Environmental Isotopes in Hydrogeology. Lewis Publishers,
560 New York (352 pp.).

561 Cravotta, C.A., (1997). Use of stable isotopes of carbon, nitrogen and Sulphur to identify
562 sources of nitrogen in surface waters in the lower Susquehanna River Basin, Pennsylvania.
563 U.S. Geological Survey Water-Supply Paper. 2497.

564 Devito, K.J., Fitzgerald, D., Hill, A.R., Aravena, R., (2000). Nitrate dynamics in relation to
565 lithology and hydrologic flow path in a river riparian zone. J. Environ. Qual. 29, 1075-1084.

566 Díaz-Cruz, M.S., Barceló, D., (2008). Trace organic chemicals contamination in ground
567 water recharge. Chemosphere 72 (3): 333-342.

568 Dillon, P., Pavelic, P., Toze, S., Rinck-Pfeiffer, S., Martin, R., Knapton, A., Pidsley, D.,
569 (2006). Role of aquifer storage in water reuse. Desalination 188 (1-3), 123-134.

570 Dogramaci, S.S., Herczeg, A.L., Schi, S.L., Bone, Y., (2001). Controls on δ34S and δ18O of
571 dissolved sulfate in aquifers of the Murray Basin, Australia and their use as indicators of flow
572 processes. Appl. Geochem. 16, 475-488

573 ENSAT (Enhancement of Soil Aquifer Treatment), (2012). Modelo hidrogeológico: Modelo
574 conceptual de flujo en el sistema de recarga de Sant Vicenç dels Horts, Barcelona: ENSAT.

575 Fox, P., et al. 2006. Advances in Soil Aquifer Treatment Research for Sustainable Water
576 Reuse. Awwa Research Foundation: Denver, 200.

577 Fukada, T., Hiscock, K., Dennis, P.F., Grischek, T., (2003). A dual isotope approach to
578 identify denitrifaction in groundwater at river-bank infiltration site. Water Res. 37, 3070-
579 3078.

580 Gibert, O., Pomierny, S., Rowe, I., Kalin, R.M., (2008). Selection of organic substrates as
581 potential reactive materials for use in a denitrification permeable reactive barrier (PRB).
582 Bioresources Technol. 99, 7587-7596.

583 Grau-Martínez, A., Torrentó, C., Carrey, R., Rodríguez-Escales, P., Domènech, C., Ghiglieri,
584 G., Soler, A., Otero, N., (2017). Feasibility of two low-cost organic substrates for inducing
585 denitrification in artificial recharge ponds: Batch and flow-through experiments. J. Contam.
586 Hydrol. 198, 48-58

587 Heberer, T., Mechlinski, A., Franck, B., Knappe, A., Massmann, G., Pekdeger, A., Fritz, B.,
588 (2004). Field studies on the fate and transport of pharmaceutical residues in bank filtration.
589 Ground Water Monit. Remediat. 24 (2), 70-77.

590 Horibe, Y., Shigehara, K., Takakuwa, Y., (1973). Isotope separation factors of carbon
591 dioxide water system and isotopic composition of atmospheric oxygen. J. Geophys. Res. 78,
592 2625-2629.

593 IAEA/WMO (2017). Global Network of Isotopes in Precipitation. The GNIP Database.
594 Accessible at: http://www.iaea.org/water

595 Iribar, V., Carrera, J., Custodio, E., Medina, A., (1997). Inverse modelling of seawater
596 intrusion in the Llobregat delta deep aquifer. J. Hydrol 198 (1-4): 226-244.

597 Kendall, C., Elliott, E.M., Wankel, S.D., (2007).Tracing anthropogenic inputs of nitrogen to
598 ecosystems. (Chapter 12). In: Michener, R.H., Lajtha, K., (Eds), Stable isotopes in Ecology
599 and Environmental Science, second ed. Blackwell Publishing, pp. 375-449.

600 Knöller, K., Vogt, C., Haupt, M., Feisthauer, S., Richnow, H.H., (2011). Experimental
601 investigation of nitrogen and oxygen isotope fractionation in nitrate and nitrite during
602 denitrification. Biogeochemistry 103, 371-384.

603 Knowles, R., (1982). Denitrification. Microbiol. Rev. 46, 43-70.

604 Köck-Schulmeyer, M., Ginebreda, A., Postigo, C., López-Serna, R., Pérez, S., Brix, R.,
605 Llorca, M., MLd Alda, Petrovic, M., Munné, A., Tirapu, L., Barceló, D., (2011). Wastewater
606 reuse in Mediterranean semi-arid areas: the impact of discharges of tertiary treated sewage
607 on the load of polar micro pollutants in the Llobregat River (NE Spain). Chemosphere 82(5):
608 670-678.

609 Krouse, H.R., Mayer, B., (2000). Sulphur and oxygen isotopes in sulphate. In: Cook, P.G.,
610 Hercseg, A.L. (Eds.), Environmnetal Tracers in Subsurface Hydrology. Kluwer Academic
611 Press, Boston, pp.195-231.

612 Lasagna, M., De Luca, D.A., (2016). The use of multilevel sampling techniques for
613 determining shallow aquifer nitrate profiles. Environ. Sci. Pollut. Res. 23 (20) 20431-20448.

614 Lehmann, M.F., Reichert, P., Bernasconi, S.M., Barbieri, A., McKenzie, J.A., (2003).
615 Modelling nitrogen and oxygen isotope fractionation during denitrification in a lacustrine
616 redox-transition zone. Geochim. Cosmochim. Acta 67, 2529-2542.

617 Li, D., Alidina, M., Ouf, M., Sharp, J.O., Saikaly, P., Drewes, J.E., (2013). Microbial
618 community evolution during simulated managed aquifer recharge in response to different
619 biodegradable dissolved organic carbon (BDOC) concentrations. Water Res. 47 (7), 2421-
620 2430.

621 Maeng, S.K., Sharma, S.K., Lekkerkerker-Teunissen, K., Amy, G.L., (2011). Occurrence and
622 fate of bulk organic matter and pharmaceutically active compounds in managed aquifer
623 recharge: a review. Water Res. 45 (10), 3015-3033.

624 Mariotti, A., Germon, J.C., Hubert, P., Kaiser, P., Letolle, R., Tardieux, P., (1981).
625 Experimental determination of nitrogen kinetic isotope fractionation: some principles,
626 illustration for the denitrification and nitrification processes. Plant Soil 62, 413-430.

627 Mariotti, A., Landreau, A., Simon, B., (1988). 15N isotope biogeochemistry and natural
628 denitrification process in groundwater application to the chalk aquifer of northern France.
629 Geochim. Cosmochim. Acta 52, 1869-1878

630 Massmann, G., Greskowiak, J., Dunnbier, U., Zuehlke, S., Knappe, A., Pekdeger, A., (2006).
631 The impact of variable temperatures on the redox conditions and the behaviour of
632 pharmaceutical residues during artificial recharge. J. Hydrol., 328 (1-2): 141- 156.

633 McIlvin, M.R., Altabet, M.A., (2005). Chemical conversion of nitrate and nitrite to nitrous
634 oxide for nitrogen and oxygen isotopic analysis in freshwater and seawater. Anal. Chem. 77,
635 5589-5595.

636 Menció, A., Mas-Pla, J., Soler, A., Regàs, O., Boy-Roure, M., Puig, R., Bach, J., Domènech,
637 C., Folch, A., Zamarona, M., Brusi, D., (2016). Nitrate pollution of groundwater; all right…,
638 but nothing else? Sci. Total Environ. 539C: 241-251.

639 Mengis, M., Schif, S.L., Harris, M., English, M.C., Aravena, R., Elgood, R.J, MacLean, A.,
640 (1999). Multiple geochemical and isotopic approaches for assessing ground water NO3
641 elimination in a riparian zone. Ground Water 37, 448-457.

642 Miller, J.H., Ela, W.P., Lansey, K.E., Chipello, P.L., Arnold, R.G., (2006). Nitrogen
643 transformations during soil-aquifer treatment of wastewater effluent-oxygen effects in field
644 studies. J. Environ. Eng. Asce 132 (10): 1298-1306.

645 Otero, N., Soler, A., Canals, A., (2008). Controls of δ34S and δ18O in dissolved sulphate:
646 learning from a detailed survey in the Llobregat River (Spain). Appl. Geochm. 23, 1166-
647 1185.

648 Otero, N., Torrentó, C., Soler, A, Menció, A., Mas-Pla, J., (2009). Monitoring groundwater
649 nitrate attenuation in a regional system coupling hydrogeology with multi-isotopic methods:
650 the case of Plana de Vic (Osona, Spain). Agric. Ecosyst. Environ. 133 (1-2), 103-113.

651 Parkhurst, DL, Appelo, CAJ (2012) Description of input and examples for PHREEQC version
652 3a computer program for speciation, batch-reaction, one-dimensional transport, and inverse
653 geochemical calculations. USGS Techniques and Methods, book 6, chap. A43, 497 p.,
654 available only at http://pubs.usgs.gov/tm/06 A43/.

655 Pauwels, H., Foucher, J.C., and Kloppmann, W. (2000). Denitrification and mixing in a schist
656 aquifer: influence on water chemistry and isotopes. Chem. Geol. 168, 307-324.

657 Pauwels, H., Ayraud-Vergnaud, V., Aquilina, L., and Molénat, J. (2010). The fate of nitrogen
658 and sulfur in hard-rock aquifers as shown by sulfate-isotope tracing. Appl. Geochem. 25,
659 105-115.

660 Pauwels, H., Kloppmann, W., Foucher, J.C., Martelat, A., and Fritsche, V. (1998). Field
661 tracer test for denitrification in a pyrite-bearing schist aquifer. Appl. Geochem. 13, 284-292.

662 Patterson, B., Shackleton, M., Furness, A., Bekele, E., Pearce, J., Linge, K., Busetti, F.,
663 Spadek, T., Toze, S., (2011). Behaviour and fate on nine recycled water trace organics
664 during managed aquifer recharge in aerobic aquifer. J. Contam. Hydrol. 122 (1-4), 53-62.

665 Pierre, C., Taberner, C., Urquiola, M.M., Pueyo, J.J., (1994). Sulphur and oxygen isotope
666 composition of sulphates in hypersaline environments, as markers of redox depositional
667 versus diagenetic changes. Mineral Mag. 58, 724-725.

668 Quevauviller, P.P., Fouillac, A.M., Grath, J., Ward, R., (2009). Groundwater monitoring,
669 Wiley, New York. ISBN: 978-0-470-74969-2.

670 Rodríguez-Escales, P., Folch, A., van Breukelen, B.M., Vidal-Gavilan, G., Sanchez-Vila, X.,
671 (2016). Modeling long term enhanced in situ biodenitrification and induced heterogeneity in
672 column experiments under different feeding strategies. J. Hydrol. 538, 127-137.

673 Ryabenko, E., Altabet, M.A., Wallace, D.W.R., (2009). Effect of chloride on the chemical
674 conversion of nitrate to nitrous oxide for δ15N analysis. Limnol. Oceanogr. 7, 545-552.

675 Schmidt, C.M., Fisher, A.T., Racz, A., Wheat, C.G., Los Huertos, M., Lockwood, B., (2012).
676 Rapid nutrient load reduction during infiltration of managed aquifer recharge in an
677 agricultural groundwater basin: Pajaro Valley, California. Hydrol. Process. 26, 2235-2247.

678 Schmidt, C.S., Richardson, DJ., Baggs, E.M., (2011). Constraining the conditions conducive
679 to dissimilatory nitrate reduction to ammonium in temperate arable soils. Soil Biol. Biochem.
680 43, 1607-1611.

681 Solà, V., (2009). Actualització hidroquímica I isotòpica dels aqüífers del Baix Llobregat per a
682 la determinació de la intrusió marina, amb consideració de la isotopia del sulfat. Tesi de
683 Màster en Hidrologia Subterrània.

684 Torrentó, C., Urmeneta, J., Otero, N., Soler, A., Viñas, M., Cama, J., (2011). Enhanced
685 denitrification in groundwater and sediments from a nitrate-contaminated aquifer after
686 addition of pyrite. Chem. Geol. 287, 90-101.

687 Utrilla, R., Pierre, C., Orti, F., Pueyo, J.J., (1992). Oxygen and sulphur isotope compositions
688 as indicators of the origin of Mesozoic and Cenozoic evaporites from Spain. Chem. Geol.
689 Isot. Geosci. 102, 229-244.

690 Valhondo, C., Carrera, J., Ayora, C., Barbieri, M., Noedler, K., Licha, T., Huerta, M., (2014).
691 Behavior of nine selected emerging trace organic contaminants in an artificial recharge
692 system supplemented with a reactive barrier. Environ. Sci. Pollut. R. 21, 11832-11843

693 Valhondo, C., Carrera, J., Ayora, Tubau, I., Martinez-Landa, L., Nödler, K., Licha, T., (2015).
694 Characterizing redox conditions and monitoring attenuation of selected pharmaceuticals
695 during artificial recharge through a reactive layer. Sci. Total Environ. 512-513, 240-250.

696 Valhondo, C., Martinez-Landa, L., Carrera, J., Hidalgo, J.J., Tubau, I., De Pourcq, K., Grau-
697 Martínez, A., Ayora, C., (2016). Tracer test modeling for local scale residence time
698 distribution characterization in an artificial recharge site. Hydrol.Earth Syst.Sci. 20, 4209-
699 4221.

700 Vanderzalm, J., Salle, C.L.G.L., Dillon, P., (2006). Fate of organic matter during aquifer
701 storage and recovery (ASR) of reclaimed water in a carbonate aquifer. Appl. Geochem. 21
702 (7), 1204-1215.

703 Vàzquez-Suñé, E., Capino, B., Abarca, E., Carrera, J., (2007). Estimation of recharge from
704 floods in disconnected stream-aquifer systems, Ground Water, 45 (5), 579-589.

705 Vitòria, L., Otero, N., Canals, A., Soler, A., (2004). Fertilizer characterization: isotopic data
706 (N, S, O, C and Sr). Environ. Sci. Technol. 38, 3254-3262.

707 Vogel, J.C., Ehhalt, D.H., (1963). The use of carbon isotopes in groundwater studies. In
708 Radioisotopes in Hydrology. Vienna: International Atomic Energy Agency, pp. 338-396.

709 Xue, D., Botte, J., De Baets, B., Accoe, F., Nestler, A., Taylor, P., Van Cleemput, O.,
710 Berglund, M., Boeckkx, P., (2009). Present limitations and future prospects of stable
711 isotopes methods for nitrate source identification in surface and groundwater. Water Res.
712 43, 1159-1170.

Figure captions

Figure 1. Upper panel: Schematic location and plan view of the Sant Vicenç dels Horts recharge system. Lower panel: Cross-section of the transect A-A'. The red diamonds show the sampling depths.

Figure 2. Operational periods of the Sant Vicenç dels Horts MAR-PRL system between January 2013 and May 2015: recharge periods (RPs, grey) and non-recharge periods (NRPs, white). The four sampling campaigns are also shown (red bars).

Figure 3. Changes in NO_3^- and NO_2^- concentrations over time in the batch experiments with compost extracted from the PRL (two-year-old reactive layer). Results of previous batch experiments with fresh commercial compost (Grau-Martínez et al., 2017) are also shown for comparison. Values and error bars represent the mean and standard deviation, respectively, for the experiments performed in triplicate.

Figure 4. Isotope analyses of the batch experiments performed with two-year-old PRL material. Slopes of the regression lines represent (α-1) for N and O.

Figure 5. $\delta^{18}O\text{-}H_2O$ vs. $\delta^{2}H\text{-}H_2O$ of samples collected in June 2013 (RP) and July 2014 (RP) from the Llobregat River, native groundwater (P1) and mixed groundwater (all the piezometers, except P1). The Local Meteoric Water Line (LMWL) and weighted mean precipitation (WMP) are also shown, as well as the groundwater samples from the Llobregat aquifer collected in an area close to the MAR pond ("Llobregat aquifer", Solà, 2009) and Llobregat river samples collected in 1998-1999 ("LB", Otero et al., 2008).

Figure. 6. Changes in the concentration of NPDOC and NO_3^- in depth-specific groundwater samples along the flow path under both RPs (a, c) and NRPs (b, d). Values for the Llobregat river samples are also shown. The size of the symbols is proportional to the corresponding concentration value. Concentrations ranged from 0.11 to 8.6 mg L^{-1} for NPDOC and from 0.01 to 19.4 mg L^{-1} for NO_3-. Concentration values are given in the Supplementary Material

(Table S3).

Figure 7. $\delta^{15}N_{NO3}$ and $\delta^{18}O_{NO3}$ of dissolved NO_3^- in the collected samples, as well as the isotope composition of the main nitrate sources: fertilizers, soil nitrate and animal manure or sewage (Vitòria et al., 2004; Kendall et al., 2007; Xue et al., 2009).

Figure 8. Estimation of the extent of NO_3^- attenuation in all the sampling campaigns, using ε values obtained from the batch experiments with two-year-old PRL material. The isotope composition of the native groundwater was used as the initial value.

Figure 9. $\delta^{18}O_{SO4}$ vs $\delta^{34}S_{SO4}$ for river, native groundwater and mixed groundwater samples collected in June 2013 and September 2013. The isotope composition of potential SO_4^{2-} sources is also shown. Values for SO_4^{2-} derived from sulfide oxidation are from Pierre et al. (1994) for disseminated pyrite in anoxic Tertiary marls that outcrop in the Llobregat River basin. Values for pig manure are taken from Otero et al. (2008) and Cravotta (1997). Soil SO_4^{2-} data are from Krouse and Mayer (2000) and fertilizer data from Vitòria et al. (2004). Gypsum values correspond to local gypsum outcrops (Utrilla et al., 1992). Sewage data are from the Igualada sewage plant (Otero et al., 2008).

Figure 10. $\delta^{13}C_{HCO3}$ vs HCO_3^- concentration for native and mixed groundwater samples collected in June 2013, September 2013 and July 2014. The dotted lines represent the range of the $\delta^{13}C_{HCO3}$ values for the native groundwater samples.

Figure 1

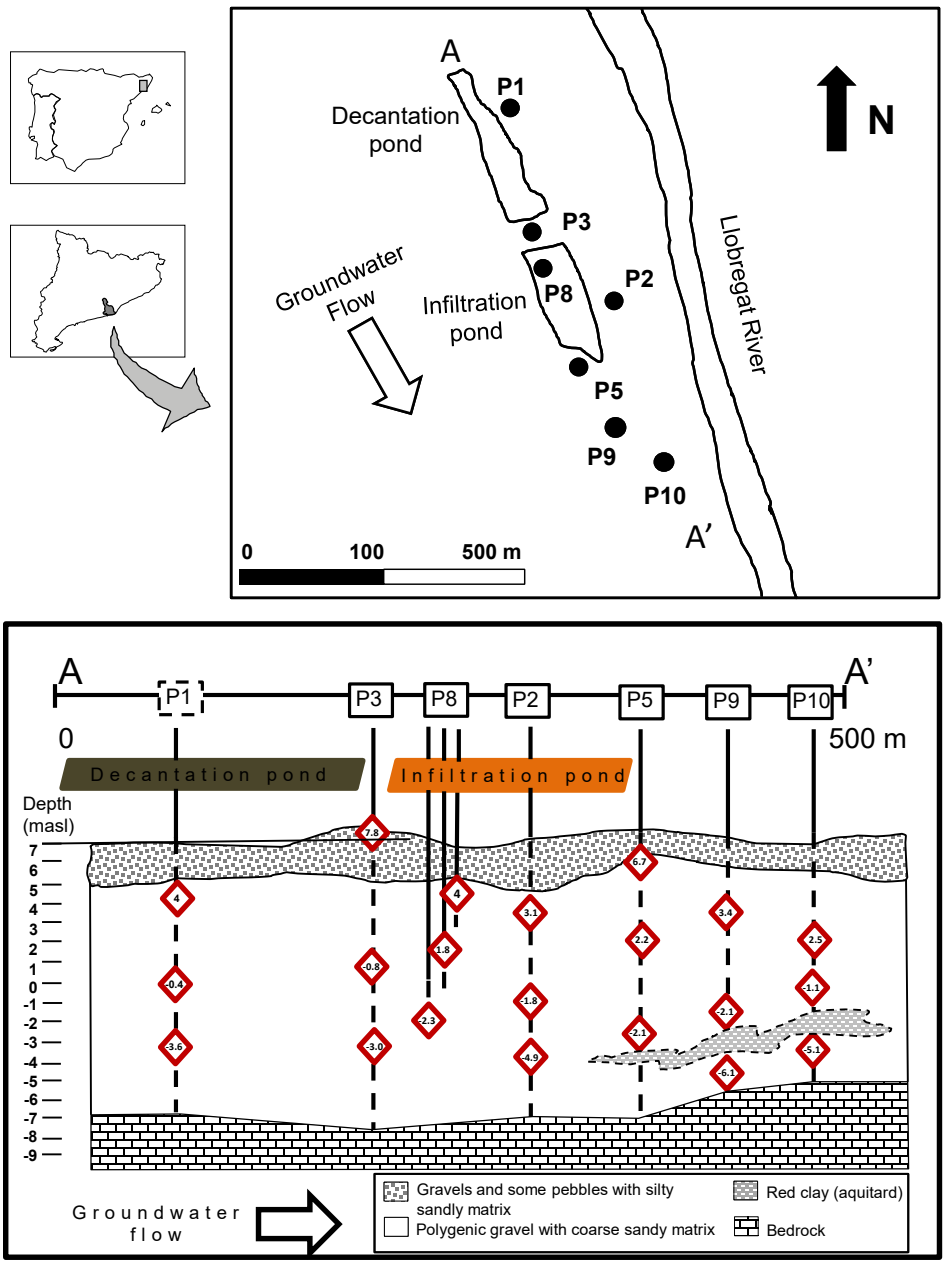
A
P1
Decantation pond
P3
P8
P2
Infiltration pond
Groundwater Flow
Llobregat River
N
P5
P9
P10
A'
0
100
500 m
A
P1
P3
P8
P2
P5
P9
P10
A'
0
500 m
Decantation pond
Infiltration pond
Depth (masl)
7
6
5
4
3
2
1
0
-1
-2
-3
-4
-5
-6
-7
-8
-9
Groundwater flow
Gravels and some pebbles with silty sandly matrix
Polygenic gravel with coarse sandy matrix
Red clay (aquitard)
Bedrock

Figure 2

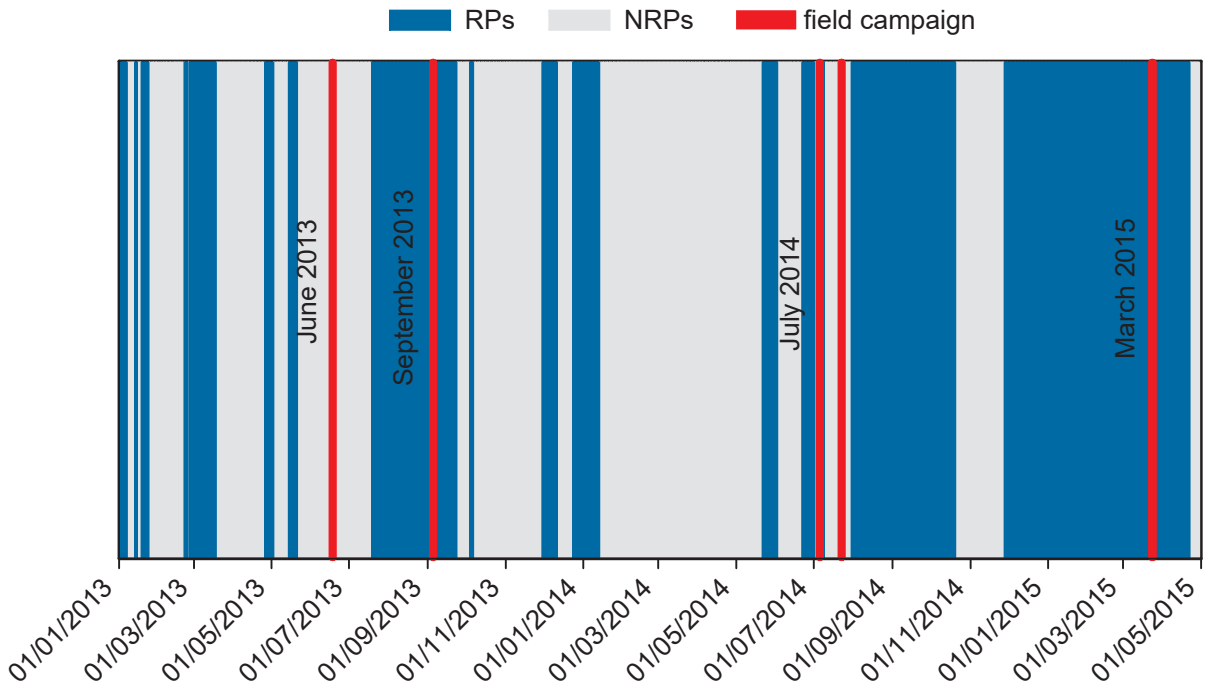
RPs
NRPs
field campaign
June 2013
September 2013
July 2014
March 2015
01/01/2013
01/03/2013
01/05/2013
01/07/2013
01/09/2013
01/11/2013
01/01/2014
01/03/2014
01/05/2014
01/07/2014
01/09/2014
01/11/2014
01/01/2015
01/03/2015
01/05/2015

Figure 3

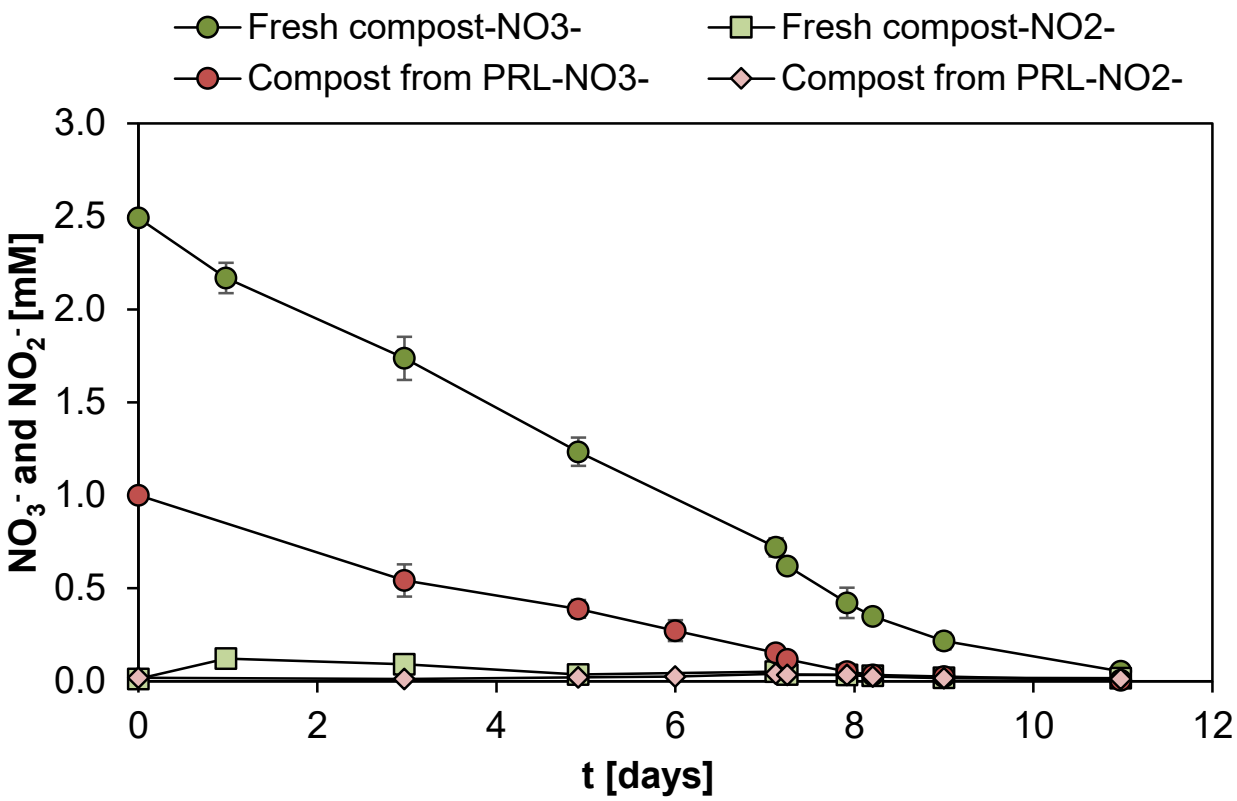
Fresh compost-NO3-
Fresh compost-NO2-
Compost from PRL-NO3-
Compost from PRL-NO2-
3.0
2.5
2.0
1.5
1.0
0.5
0.0
0
2
4
6
8
10
12
t [days]
NO3- and NO2- [mM]

Figure 4

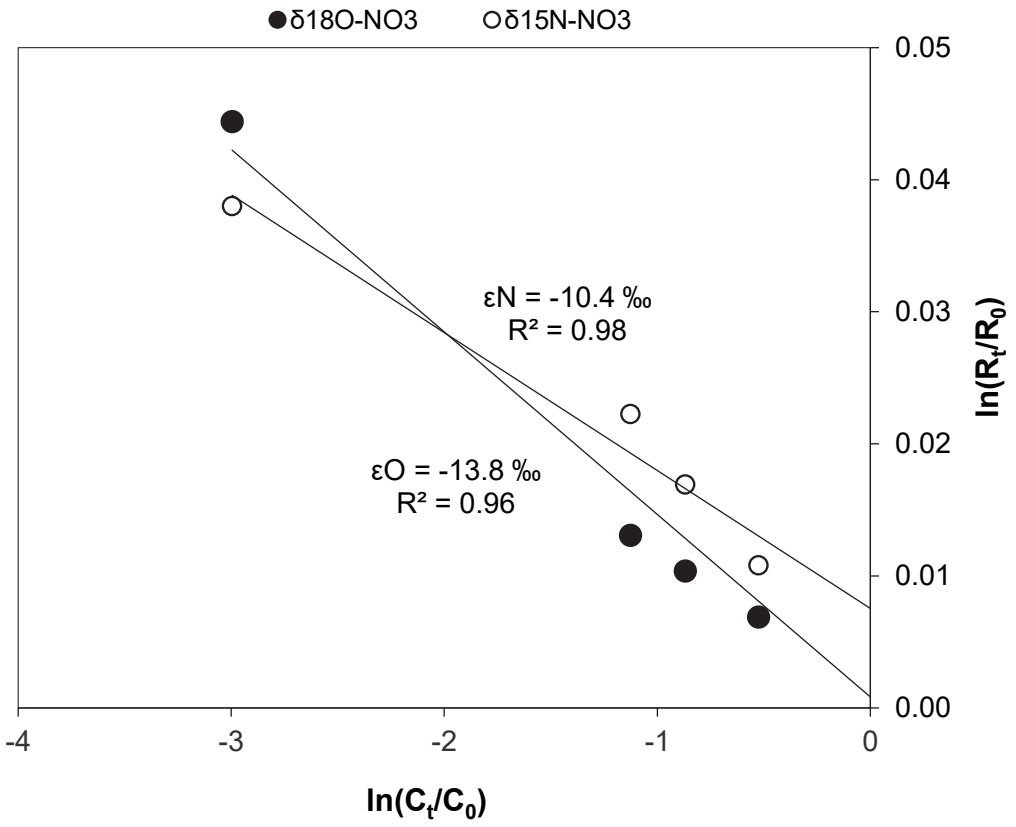
●δ18O-NO3
○δ15N-NO3
εN = -10.4 ‰
R² = 0.98
εO = -13.8 ‰
R² = 0.96
0.05
0.04
0.03
0.02
0.01
0.00
-4
-3
-2
-1
0
ln(Ct/C0)
ln(Rt/R0)

Figure 5

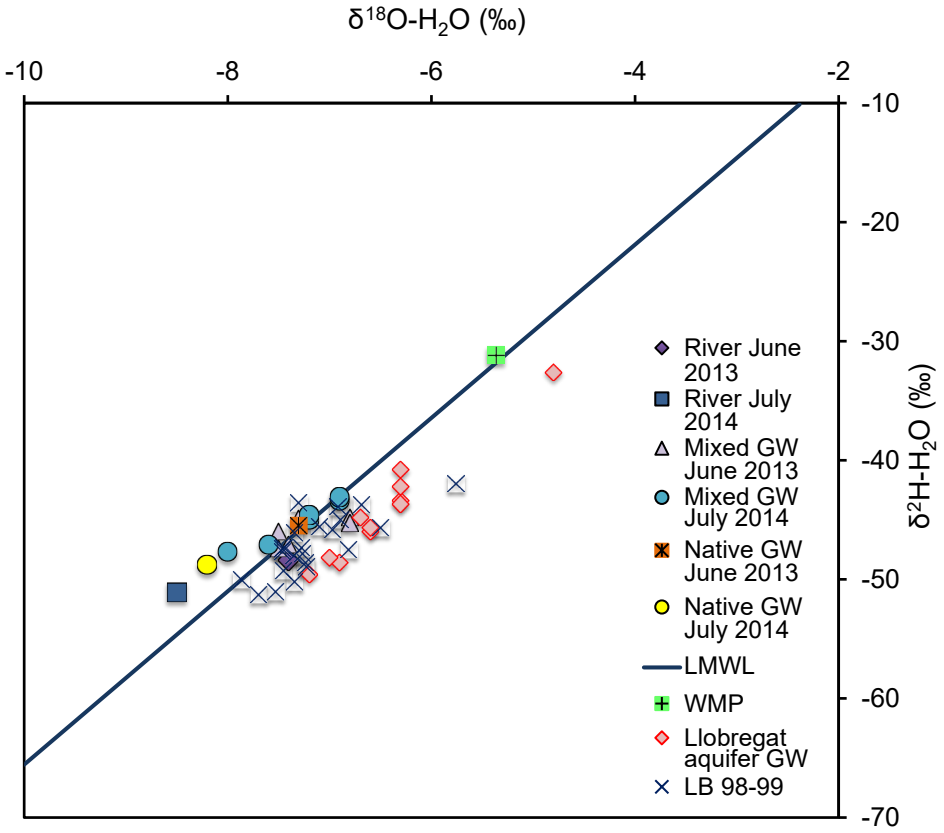
δ18O-H2O (‰)
-10
-8
-6
-4
-2
-10
-20
-30
-40
-50
-60
-70
δ2H-H2O (‰)
River June 2013
River July 2014
Mixed GW June 2013
Mixed GW July 2014
Native GW June 2013
Native GW July 2014
LMWL
WMP
Llobregat aquifer GW
LB 98-99

Figure 6

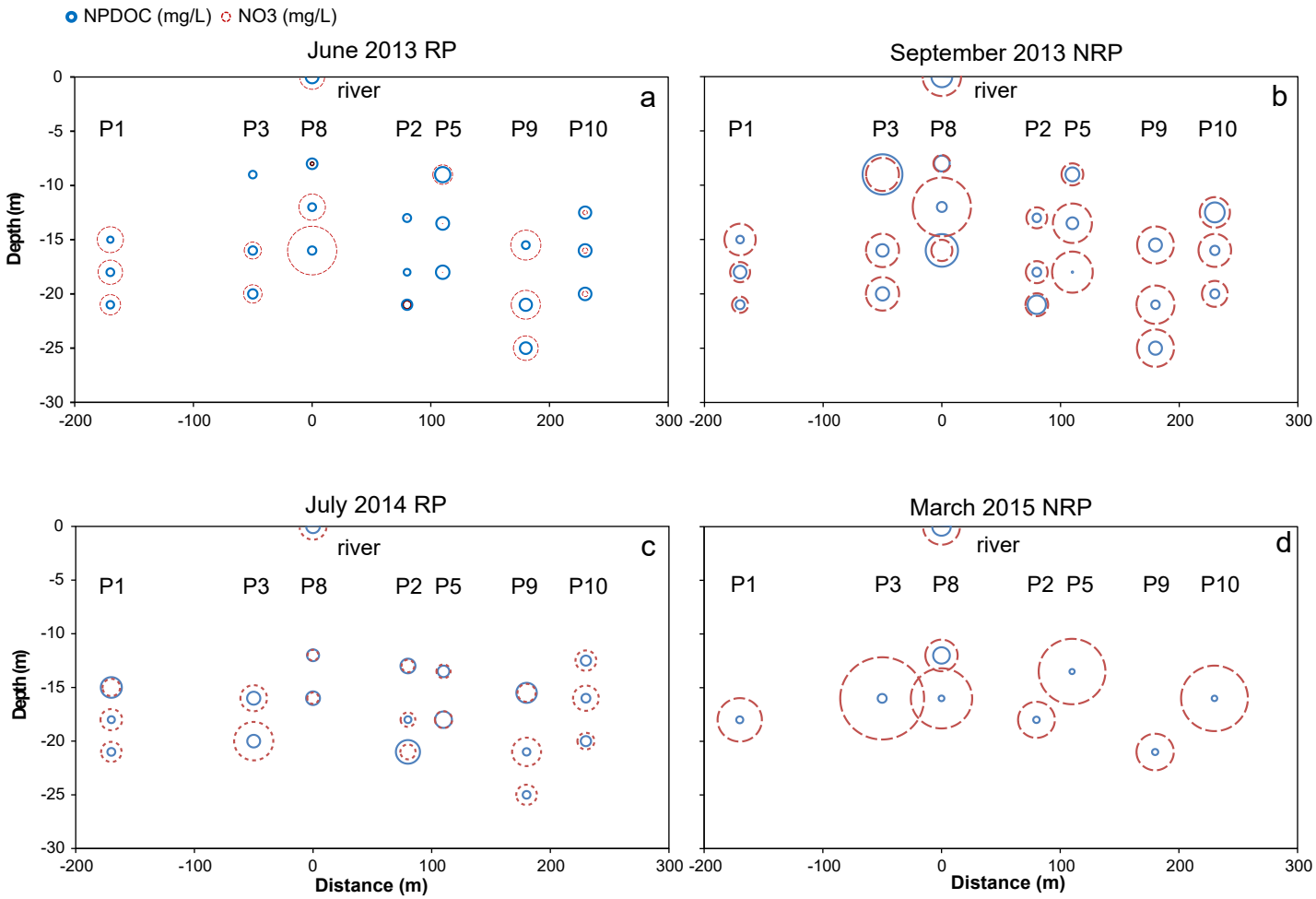
NPDOC (mg/L)
NO3 (mg/L)
June 2013 RP
September 2013 NRP
July 2014 RP
March 2015 NRP
river
a
b
c
d
P1
P3
P8
P2
P5
P9
P10
Depth (m)
Distance (m)
0
-5
-10
-15
-20
-25
-30
-200
-100
0
100
200
300

Figure 7

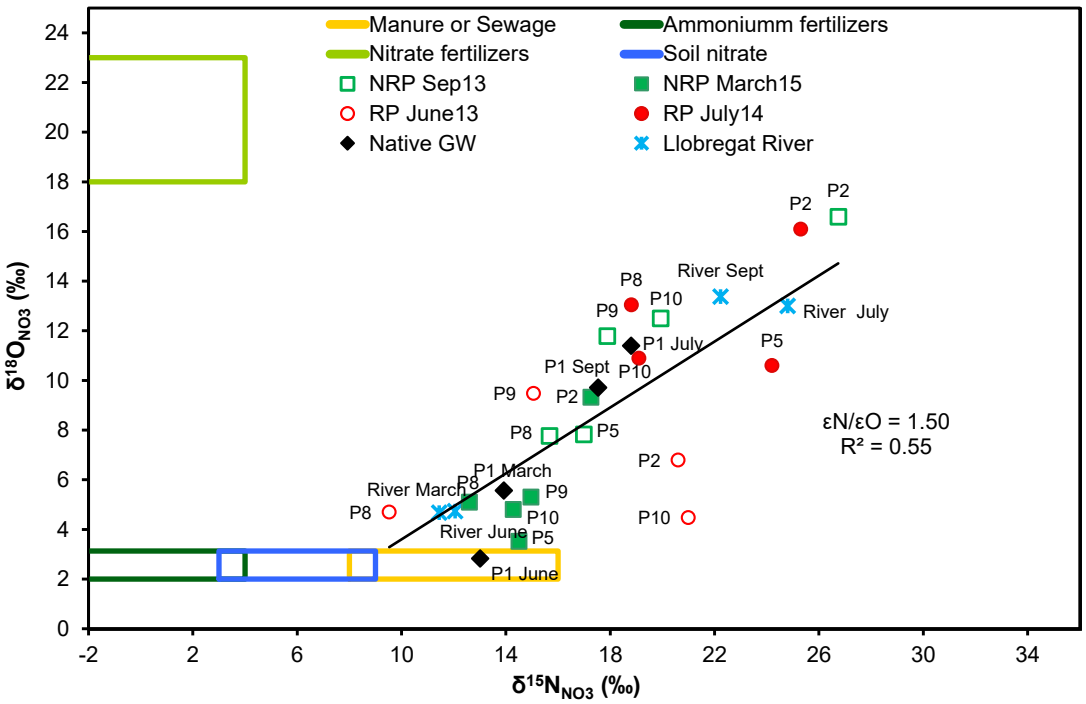
Manure or Sewage
Ammoniumm fertilizers
Nitrate fertilizers
Soil nitrate
NRP Sep13
NRP March15
RP June13
RP July14
Native GW
Llobregat River
δ18ONO3 (‰)
δ15NNO3 (‰)
εN/εO = 1.50
R² = 0.55
P2
P8
P10
P9
P1 July
P5
P1 Sept
River Sept
River July
P1 March
River March
River June
P1 June

Figure 8

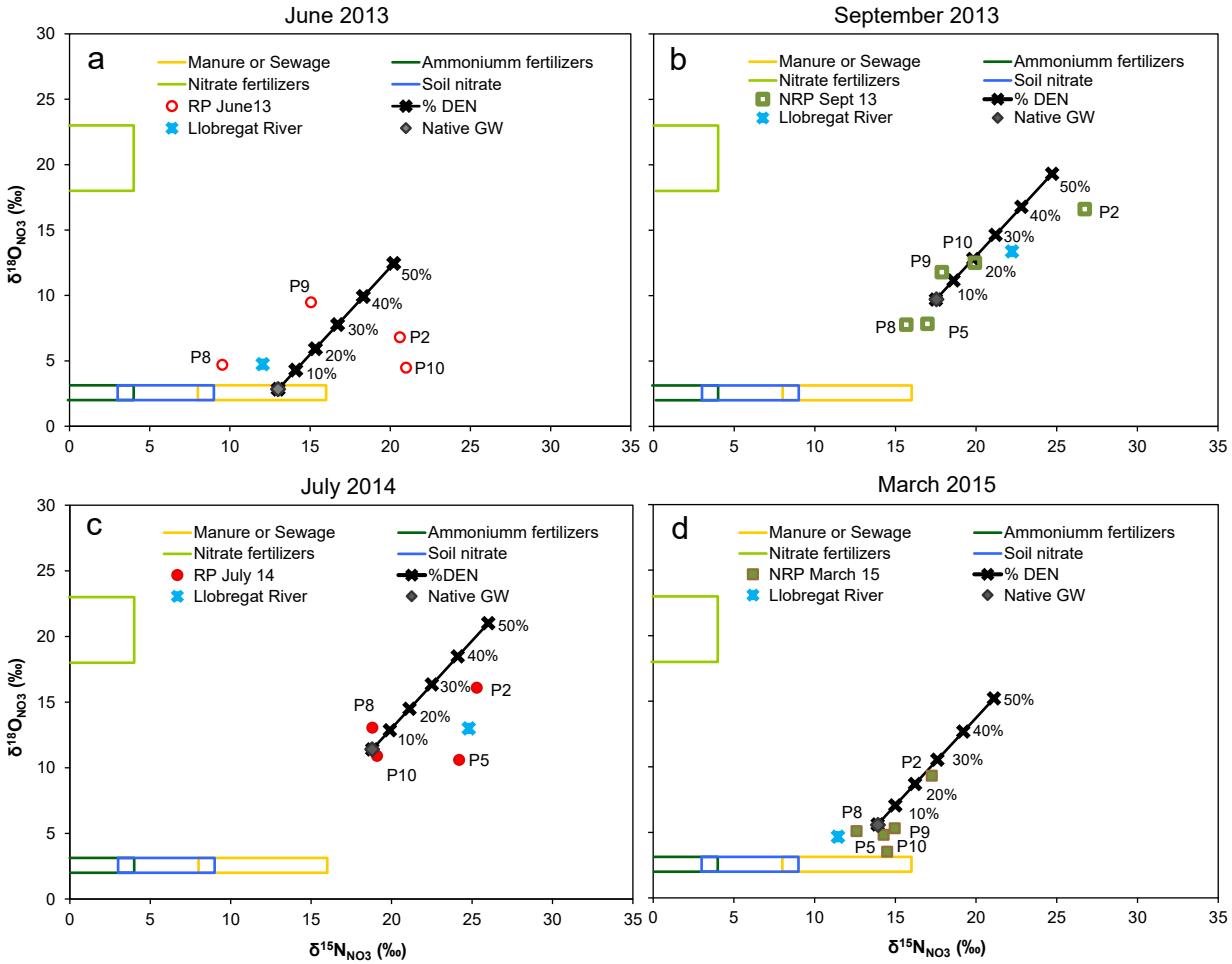
June 2013
a
Manure or Sewage
Nitrate fertilizers
RP June13
Llobregat River
Ammoniumm fertilizers
Soil nitrate
% DEN
Native GW
P9
P8
P2
P10
50%
40%
30%
20%
10%
September 2013
b
Manure or Sewage
Nitrate fertilizers
NRP Sept 13
Llobregat River
Ammoniumm fertilizers
Soil nitrate
% DEN
Native GW
P2
P10
P9
P8
P5
July 2014
c
Manure or Sewage
Nitrate fertilizers
RP July 14
Llobregat River
Ammoniumm fertilizers
Soil nitrate
%DEN
Native GW
P8
P2
P5
P10
March 2015
d
Manure or Sewage
Nitrate fertilizers
NRP March 15
Llobregat River
Ammoniumm fertilizers
Soil nitrate
% DEN
Native GW
P2
P8
P9
P5
P10
δ18ONO3 (‰)
δ15NNO3 (‰)

Figure 9

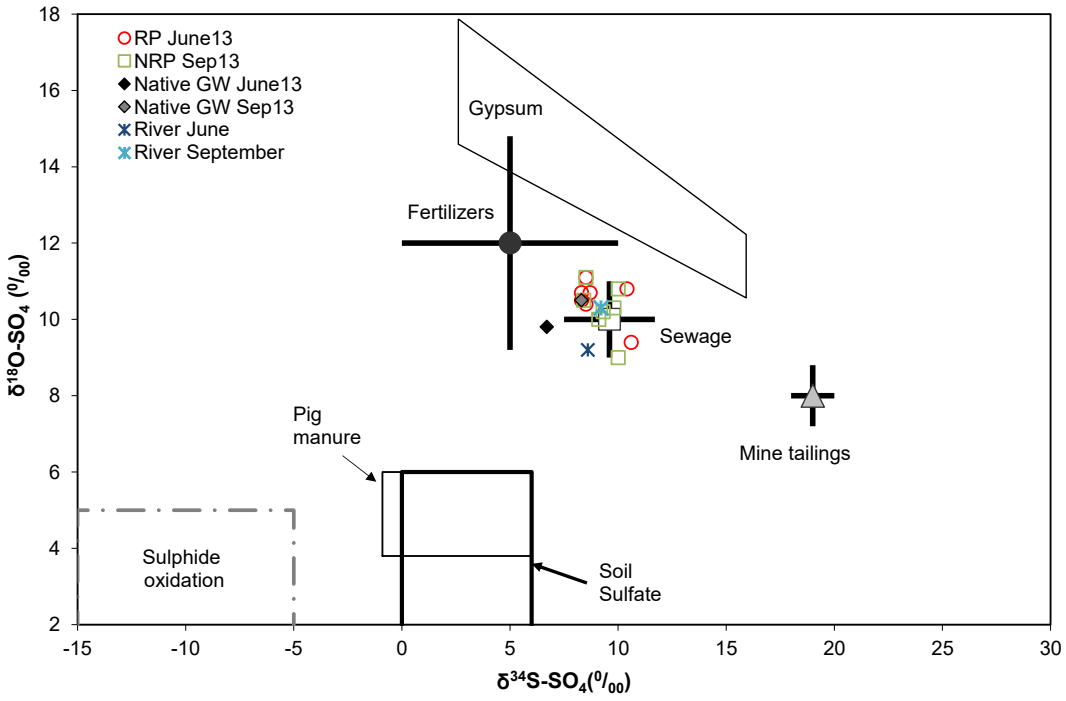
RP June13
NRP Sep13
Native GW June13
Native GW Sep13
River June
River September
Gypsum
Fertilizers
Sewage
Mine tailings
Pig manure
Sulphide oxidation
Soil Sulfate
δ18O-SO4 (0/00)
δ34S-SO4(0/00)
18
16
14
12
10
8
6
4
2
-15
-10
-5
0
5
10
15
20
25
30

Figure 10

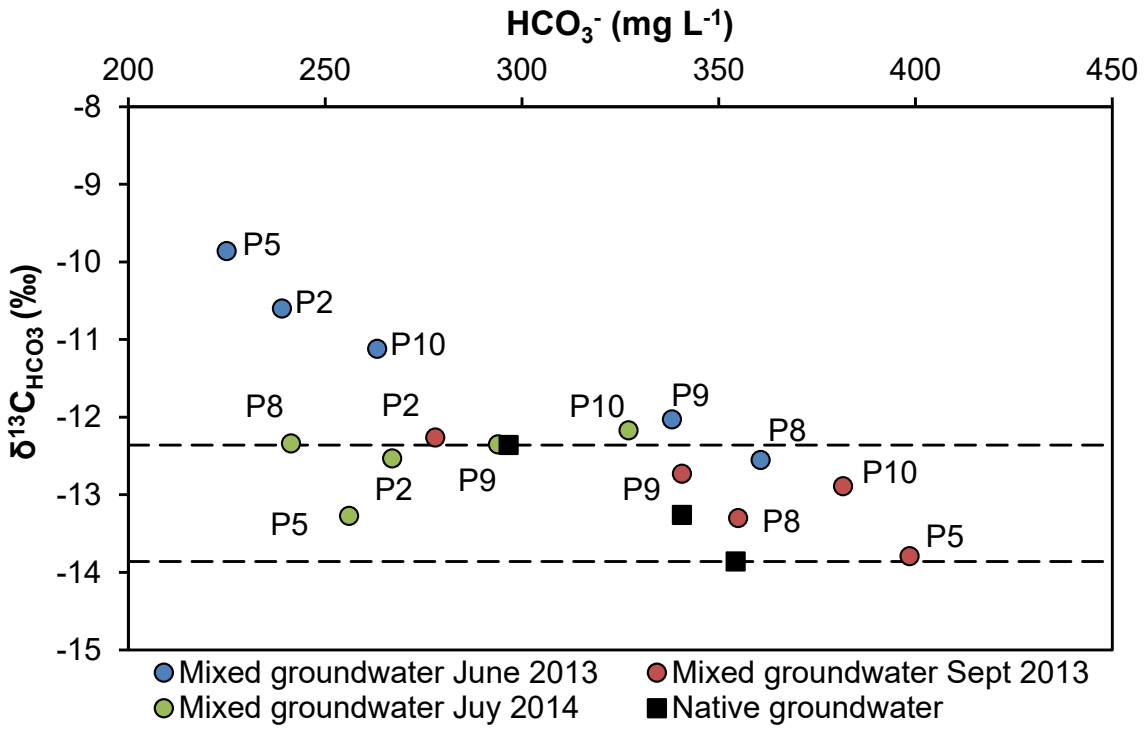
HCO3- (mg L-1)
200
250
300
350
400
450
-8
-9
-10
-11
-12
-13
-14
-15
δ13CHCO3 (‰)
P5
P2
P10
P8
P2
P10
P9
P8
P2
P9
P9
P10
P5
P8
P5
Mixed groundwater June 2013
Mixed groundwater Sept 2013
Mixed groundwater Juy 2014
Native groundwater